Parabolic temporal profiles of non-spanning avalanches and their importance for ferroic switching

X. He, X. Ding, J. Sun, and E. K. H. Salje

Citation: Applied Physics Letters **108**, 072904 (2016); doi: 10.1063/1.4942387
View online: http://dx.doi.org/10.1063/1.4942387
View Table of Contents: http://scitation.aip.org/content/aip/journal/apl/108/7?ver=pdfcov
Published by the AIP Publishing

Parabolic temporal profiles of non-spanning avalanches and their importance for ferroic switching

X. He,[1] X. Ding,[1,a)] J. Sun,[1] and E. K. H. Salje[1,2,a)]
[1]State Key Laboratory for Mechanical Behavior of Materials, Xi'An Jiaotong University, Xian 710049, People's Republic of China
[2]Department Earth Sciences, University of Cambridge, Cambridge CB2 3EQ, England

(Received 6 January 2016; accepted 6 February 2016; published online 17 February 2016)

Computer simulation of a ferroelastic switching process shows avalanche formation with universal averaged temporal avalanche profiles $\langle J(t)\rangle$, where J(t) is the avalanche "amplitude" at time t. The profiles are derived for the three most commonly used "jerk"-singularities, namely, the total change of the potential energy U via $J(t) = (dU(t)/dt)^2$, the energy drop $J(t) = -dU/dt$, and the stress drop $J(t) = -d\tau_{xy}/dt$. The avalanches follow, within the time resolution of our modeling, a universal profile $J(t)/J_{max} = 1 - 4(t/t_{max} - 0.5)^2$ in the a-thermal regime and the thermal regime. Broadening of the profiles towards a 4th order parabola arises from peak overlap or peak splitting. All profiles are symmetric around $t/t_{max} = 0.5$ and are expected to hold for switching processes in ferroic materials when the correlations during the avalanche are elastic in origin. High frequency applications of ferroic switching are constrained by this avalanche noise and its characteristic temporal distribution function will determine the bandwidth of any stored or transmitted signal.
[http://dx.doi.org/10.1063/1.4942387]

Domain switching in piezoelectric, ferroelectric, ferroelastic, and magnetic materials usually involves fine structures on a nano-meter scale that, on aggregate, constitute the macroscopic switch (review in Ref. 1). A typical example is the lateral movement of a ferroelectric domain wall, which is composed of moving kinks in the wall.[2] The kink size extends over few atomic layers. Most macroscopic observations will identify only the lateral domain wall movement as a time averaged process, while the elementary step of the kink movement is visible only in high time-resolution experiments such as acoustic emission (AE) measurements.[3] With the advent of experimental methods such as femtosecond spectroscopy, the focus of research shifted from the description of averaged quantities to processes that include the local jerks. Alternatively, computer simulations have revealed that most fine structures lead to "jerky" movements and heterogeneities on a sufficiently short time scale.[4–9] We use the term "jerk" as an experimental manifestation in any physical observable of an avalanche. High frequency applications of ferroic materials may rely on jerk-infested switching processes for data storage and transmission. Both processes are possible only outside the frequency interval of the avalanche noise so that the avalanche characteristics are an essential parameter for all high frequency device applications.

Jerks often combine to produce crackling noise[10–14] and the formation of avalanches where each nano-structural movement triggers others with bursts of activities and waiting times between avalanches. In this paper, we distinguish carefully between the observation of short-time singularities, which are termed "jerks" and the underlying physical process, namely, the formation of avalanches. The experimental investigation of avalanches is often based on the observation of a multitude of "jerks," which defines the Probability Distribution Function, PDF, of the avalanche. The distinction between the observable "jerk" and the underlying physical object "avalanche" is necessary because not all "jerks" are signatures of avalanches but may be artifacts (e.g., laboratory noise, sample vibrations), which need to be eliminated before one can discuss avalanche statistics based on "jerks" measurements. Here we are concerned with jerks as manifestations of avalanches. The probability $P(J)$ of a jerk J to occur is typically power law distributed $P(J) \sim J^{-\varepsilon}F(J)$, where $F(J)$ is some (exponential) non-universal cut-off function.[15] Similar power law distributions exist for waiting times between avalanches.[16] Avalanches in most disordered materials are described by a narrow range of dynamical exponents both for the energy distributions and the waiting times between avalanches. The avalanches are hence related to those elementary processes that lead to domain switching and represent the intrinsic noise of the switching process (even in the absence of defects). This noise will ultimately limit the applications of ferroic devices and will curtail high frequency applications of domain switching: any hysteretic switching consists of avalanches of domain movements, which become experimentally visible at sufficiently short time scales. The power law dependence of the avalanche parameters means that individual jerks will have durations and waiting times (between subsequent jerks) without any scale dependence and an extremely broad distribution. The avalanches generate "inevitable" noise of the switching process, which can be described using statistical concepts, which are partly described in this paper.

a)Authors to whom correspondence should be addressed. Electronic addresses: ekhard@esc.cam.ac.uk and dingxd@mail.xjtu.edu.cn

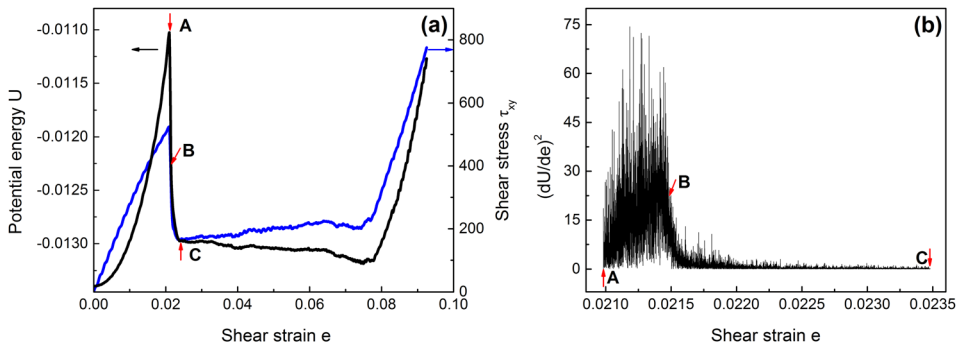

FIG. 1. (a) Potential energy U (black line) and shear stress (blue line) versus external shear strain e at T = 1 K. (b) Corresponding jerk distributions $(dU/de)^2$ between the point A and C in (a). The avalanches cover two regimes (A-B and B-C), spanning avalanches are found in A-B while B-C contains only local switching avalanches. Avalanches in the regime A-B depend strongly on the sample size but not in the regime B-C.

Avalanches are largely scale invariant and are described by statistical quantities.[15] Jerks were observed in heat flux measurements (thermal jerks),[17] AE (acoustic jerks) and slip avalanches in metallic glasses,[18–24] spikes in the polarization (electric jerks), and Barkhausen noise[2,14] (magnetic jerks). Each jerk signal is characterized by fairly random, often jagged profiles so that the question arises: is the time evolution predictable if one considers the averaged profiles? Averaging needs to extend over the two probabilistic parameters of the avalanche, namely, its duration and amplitude. The duration is the time between the start and the end of each avalanche so that duration depends on the threshold of the jerk energy. The amplitude of each jerk profile is defined as its maximum. All normalized profiles (time and amplitude) are numerically averaged so that each switching process with a multitude of jerks is characterized by one single characteristic "jerk profile" (further details in Ref. 25). These profiles are then compared between avalanches under different thermodynamic conditions, sizes, and boundary conditions.

The mean-field hypothesis is that the characteristic profiles have parabolic profiles[25] and that they are largely independent of temperature. They may strongly reflect size and boundary effects (e.g., thin films on substrates). Few papers have addressed this problem previously. Averaged jerk profiles have been determined so far for slip avalanches in metallic glasses,[25] deformations during crystal plasticity,[26] in granular materials,[27] shear bands,[28] and superconductors.[29] Simulations of jerk profiles in ferroelastic materials seem to confirm the parabola hypothesis[30] although this work combined spanning avalanches ("large avalanches") at yield points with more local switching avalanches ("small avalanches"). A similar distinction was made between "small slip avalanches" and "large slip avalanches" in metallic glasses[25] and related to different physical processes underlying the small and large slip process. It is the purpose of this paper to show that the parabola hypothesis is indeed correct for switching in ferroic materials with strong elastic correlations that proceeds via "small avalanches."

The computer simulations are based on the standard ferroelastic model;[31] the potential energy $U(r)$ is composed of three interactions, the first-nearest atomic interactions $U_{NN} = 10(r-1)^2 (0.8 \le r < 1.288)$, the second-nearest atomic interactions $U_{NNN} = -10(r-\sqrt{2})^2 + 2000(r-\sqrt{2})^4$ $(1.288 \le r < 1.54)$, and the third-nearest interactions $U_{NNNN} = -(r-2)^4$ $(1.54 \le r < 2.2)$, where r is atomic distance vector. The shear angle is the order parameter in this model. The equilibrium unit cell is a parallelogram with a shear angle of 4°. We set the equilibrium lattice constant a = 1 Å and atomic mass M = 100 amu. Free boundary conditions are adopted and twinned sandwich structure containing two pre-existing horizontal twin boundaries (HTBs) as the initial configuration.

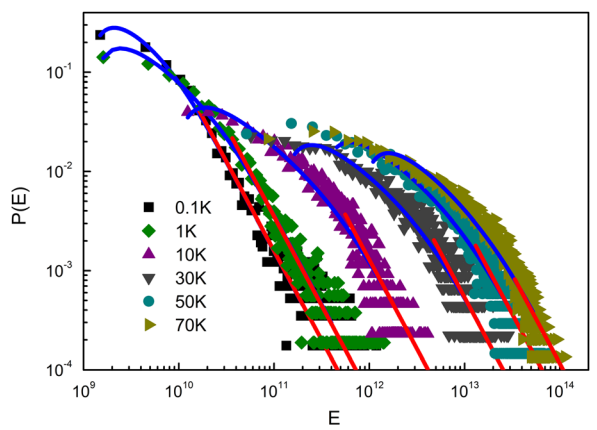

FIG. 2. The probability distribution of the jerk energy P(E) for a large temperatures range from 0.1 K to 70 K. Power law regions are shown by red lines; blue lines indicate the exponential regions.

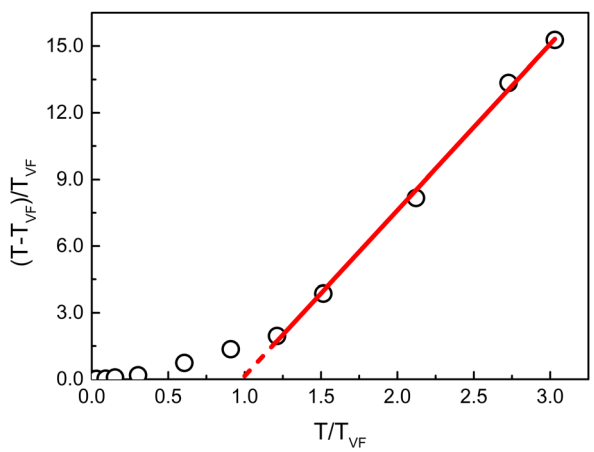

FIG. 3. Phase diagram of the distribution functions for the pattern formation as a function of temperature. The Vogel-Fulcher parameter $(T-T_{VF})/T_{VF}$ is zero in the a-thermal regime and increases linearly with T at $T > T_{VF}$ where avalanches are thermally activated. The crossover between the power law regime and the thermally activated regime occurs near $T = T_{VF}$.

The size of our 2D simulation is 500a × 502a. The ratio of the height of the switchable intermediate layer to the total sample is fixed to be 0.5. The system was first relaxed with a conjugate gradient refinement procedure at the beginning of the simulations. Then molecular dynamics (MD) was performed to anneal the configuration at a large range of given temperature for 5×10^6 time steps. No microstructures developed, except for some surface relaxations, during this procedure. Finally, at the top and bottom several layers of atoms were fixed rigidly and then sheared with a constant shear strain rate 5×10^7 1/s in a canonical ensemble. All MD simulations were performed with the LAMMPS code,[32] and the Nosé-Hoover thermostat[33,34] was used to hold the sample's temperature in constant.

The external strain e is the field variable (∼"hard boundary conditions"), which increases with constant strain rate. The jerk signal J is defined in this paper in three different ways using the conventions of previous work. First, as the square of the time derivative of the potential energy U,[31,35] $J(t) = (dU/dt)^2 \sim (dU/de)^2$. Here we characterize time t by the external strain e as the strain rate is constant. Second, we calculate the avalanche profile of the energy drop $J(t) = -dU/dt \sim -dU/de$, and third, the shear stress drop $J(t) = -d\tau_{xy}/dt \sim -d\tau_{xy}/de$. The simulated avalanches cover two regimes as shown in Fig. 1 for U and $(dU/de)^2$. During the yield event, very intense avalanches include many spanning avalanches, which penetrate the entire sample (A-B). They do not represent switching avalanches and their statistical properties depend strongly on the sample size. They are dismissed from our statistical analysis. Avalanches related to local switches (∼small avalanches) dominate the regime between the points B and C. We consider only these avalanches in the analysis.

Avalanches are known to be a-thermal at low temperatures and become strongly temperature dependent at high temperatures.[31] We first reproduce this result using our potential (in our potential the cut-off rages are continuous, while they were discontinuous in a previous potential,[2,7–9] namely, U_{NN}: $0.8 < r < 1.2$; U_{NNN}: $1.207 \leq r < 1.621$; U_{NNNN}:1.8 $r < 2.2$) restricting the analysis to avalanches in

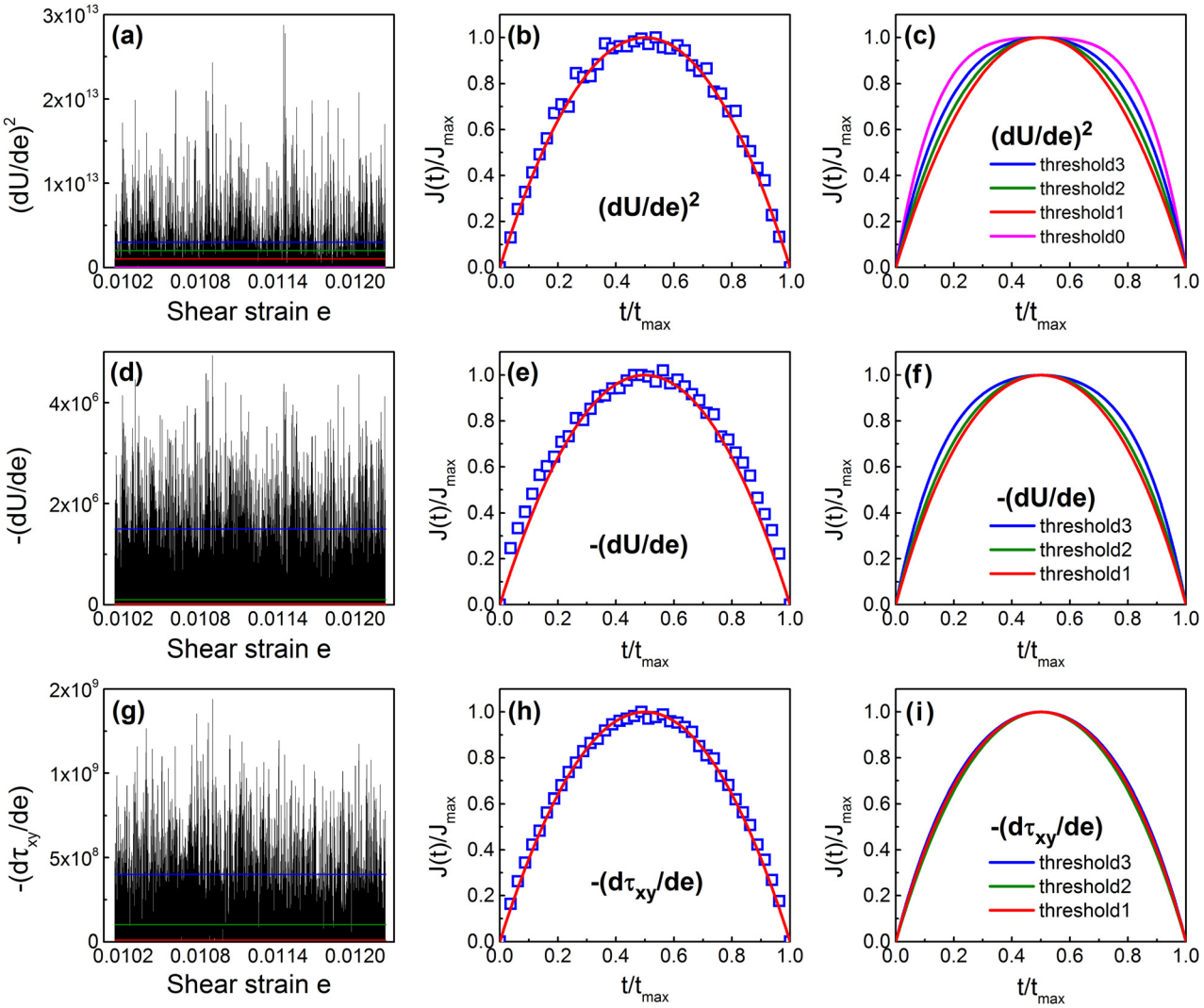

FIG. 4. Jerk spectrum of $(dU/de)^2$ (a), $-dU/de$ (d), and $-d\tau_{xy}/de$ (g) at 30 K with various threshold levels. Only peaks above a given threshold were used to calculate the temporal jerk profiles. Temporal jerk profiles of $(dU/de)^2$ (b), $-dU/de$ (e), and $-d\tau_{xy}/de$ (h) show parabolic avalanche profiles: $J(t)/J_{max} = 1 - 4(t/t_{max} - 0.5)^2$ (the red line in (b), (c), (e), (f), (h), and (i)). The change of temporal jerk profiles of $(dU/de)^2$ (c), $-dU/de$ (f), and $-d\tau_{xy}/de$ (i) with changing threshold tend towards a 4th order parabola which arises from peak overlap at very low threshold (threshold 0 in (c)) or peak splitting at high threshold (threshold 2 and 3 in (c), (f), and (i)).

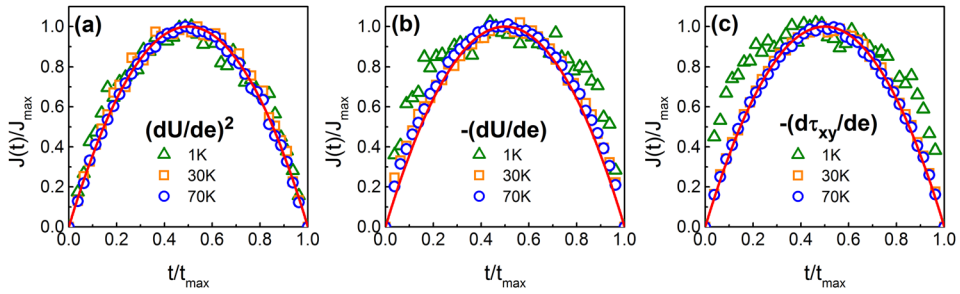

FIG. 5. Change of temporal jerk profiles of $(dU/de)^2$ (a), $-dU/de$ (b), and $-d\tau_{xy}/de$ (c) with temperature. The red line in (a), (b), and (c) shows the parabolic fitting: $J(t)/J_{max} = 1 - 4(t/t_{max} - 0.5)^2$.The profile of $(dU/de)^2$ is not sensitive to the temperature. The profiles of $-dU/de$ (b) and $-d\tau_{xy}/de$ (c) are flatter at low temperature (triangle points), and become insensitive to temperature when the temperature of system is higher than 30 K.

the regime B-C. The PDF over a large range of temperatures is shown in the double-logarithmic plots in Fig. 2. Large power law regimes are seen for low temperatures (0.1 K and 1 K), while the exponential cut-off becomes dominant at higher temperatures. We indicated the power law regions by red lines; black lines show the exponential regions. The crossover between the power law regime and the thermally activated regime near T_{VF} shifts to higher energies with increasing temperature.[31] The inverse slope of the linear-logarithmic plots identifies the activation energy of thermal jerks. These jerks follow Vogel-Fulcher statistics[31] with the characteristic crossover of $(T-T_{VF})/T_{VF}$ near the Vogel-Fulcher temperature T_{VF} (Fig. 3). The Vogel-Fulcher parameter $(T-T_{VF})/T_{VF}$ is zero in the a-thermal regime and increases linearly with T at $T > T_{VF}$. This result agrees with the simulations in Refs. 30 and 31 using different potentials, which shows that the results are fairly robust as long as the interactions are long-ranging.

The temporal avalanche profiles were now determined by normalizing the duration and the peak intensities of all three jerk quantities; the average profiles are then calculated using the superposition of >770 jerks (with more than 5 points in each jerk). As expected, the temporal profiles depend somewhat on the lower threshold of the jerk spectra (see Fig. 4(a)). Very low thresholds include overlaps between small peaks. The small peak profiles are hence not always profiles of single events.[15] Thresholds at a higher level hold the danger that the peak duration is underestimated which can also equally falsify the temporal profile. To test the proper use of the threshold, we choose at least 3 thresholds for $(dU/de)^2$ (Fig. 4). The peak profiles are shown in Figs. 4(b) and 4(c). We then calculated the avalanche profiles of the energy drops $-dU/de$ (Figs. 4(d)–4(f)) and the shear stress drops $-d\tau_{xy}/de$ (Figs. 4(g)–4(i)). The best fit for all avalanche profiles is a universal parabola with $J(t)/J_{max} = 1 - 4(t/t_{max} - 1/2)^2$ for immediate threshold (threshold 1 in Fig. 4) in the a-thermal regime (1 K in Fig. 5) and the thermal regime (70 K in Fig. 5). This confirms the hypothesis that the avalanche profiles are essentially independent of temperature. The quadratic parabola will change to 4th order parabola in the case of very low threshold where peak overlap is severe, or in the case of high threshold where peak splitting becomes obvious. This broadening of avalanche profiles with changing threshold is consistent with the results in bulk metallic glasses where increasing avalanche duration leads to flatter avalanche profiles.[25] In addition, we notice that the scaling of $(dU/de)^2$ is better defined than the scaling of $-dU/de$ and $-d\tau_{xy}/de$. The avalanche profiles of $-dU/de$ (d) and $-d\tau_{xy}/de$ are slightly flatter than for $(dU/de)^2$ at low temperature (triangle points in Fig. 5(b) and 5(c)) and only become insensitive to temperature when the temperature of system is higher than 30 K. However, the number of avalanches is small at lower temperatures so that the broadening may be statistically less significant. The averaged profiles are always symmetric in our simulations.

In summary, we identify the quadratic parabola as being the universal profile for ferroelastic switching avalanches in the standard ferroelastic model and may assume that most ferroelastic switching processes will follow this profile.

X.H., X.D., and J.S. are grateful to NSFC (51320105014, 51321003, 51231008) for financial support. E.K.H.S. thanks EPSRC (EP/K009702/1) for financial support.

[1]T. M. Shaw, S. Trolier-McKinstry, and P. C. McIntyre, Annu. Rev. Mater. Sci. **30**, 263 (2000).
[2]E. K. H. Salje, X. Wang, X. Ding, and J. Sun, Phys. Rev. B **90**, 064103 (2014).
[3]E. Dul'kin, E. K. H. Salje, O. Aktas, R. W. Whatmore, and M. Roth, Appl. Phys. Lett. **105**, 212901 (2014).
[4]K. A. Dahmen, Y. Ben-Zion, and J. T. Uhl, Phys. Rev. Lett. **102**, 175501 (2009).
[5]O. Perković, K. A. Dahmen, and J. P. Sethna, Phys. Rev. B **59**, 6106 (1999).
[6]E. K. H. Salje, X. Ding, Z. Zhao, and T. Lookman, Appl. Phys. Lett. **100**, 222905 (2012).
[7]X. Ding, Z. Zhao, T. Lookman, and E. K. H. Salje, Adv. Mater. **24**, 5385 (2012).
[8]X. Ding, T. Lookman, Z. Zhao, J. Sun, and E. K. H. Salje, Phys. Rev. B **87**, 094109 (2013).
[9]Z. Zhao, X. Ding, T. Lookman, J. Sun, and E. K. H. Salje, Adv. Mater. **25**, 3244 (2013).
[10]J. P. Sethna, K. A. Dahmen, and C. R. Myers, Nature **410**, 242 (2001).
[11]G. Tsekenis, N. Goldenfeld, and K. A. Dahmen, Phys. Rev. Lett. **106**, 105501 (2011).
[12]M. J. Alavaa, P. K. V. V. Nukala, and S. Zapperi, Adv. Phys. **55**, 349 (2006).
[13]D. Bonamy, S. Santucci, and L. Ponson, Phys. Rev. Lett. **101**, 045501 (2008).
[14]F. Colaiori, Adv. Phys. **57**, 287 (2008).
[15]E. K. H. Salje and K. A. Dahmen, Annu. Rev. Condens. Matter Phys. **5**, 233 (2014).
[16]J. Baró, Á. Corral, X. Illa, A. Planes, E. K. H. Salje, W. Schranz, D. E. Soto-Parra, and E. Vives, Phys. Rev. Lett. **110**, 088702 (2013).
[17]M. C. Gallardo, J. Manchado, F. J. Romero, J. del Cerro, E. K. H. Salje, A. Planes, E. Vives, R. Romero, and M. Stipcich, Phys. Rev. B **81**, 174102 (2010).

[18]E. K. H. Salje, E. Dul'kin, and M. Roth, Appl. Phys. Lett. **106**, 152903 (2015).
[19]A. Saxena and A. Planes, *Mesoscopic Phenomena in Multifunctional Materials* (Springer, Berlin, 2014).
[20]E. Vives, J. Ortın, L. Manosa, I. Rafols, R. Perez-Magrane, and A. Planes, Phys. Rev. Lett. **72**, 1694 (1994).
[21]J. Baro, S. Dixon, R. S. Edwards, Y. Fan, D. S. Keeble, L. Manosa, A. Planes, and E. Vives, Phys. Rev. B **88**, 174108 (2013).
[22]E. K. H. Salje, J. Koppensteiner, M. Reinecker, W. Schranz, and A. Planes, Appl. Phys. Lett. **95**, 231908 (2009).
[23]Z. Balogh, L. Daroczi, L. Harasztosi, D. L. Beke, T. A. Lograsso, and D. L. Schlagel, Mater. Trans. **47**, 631 (2006).
[24]K. S. Ryu, H. Akinaga, and S. C. Shin, Nat. Phys. **3**, 547 (2007).
[25]J. Antonaglia, W. J. Wright, X. Gu, R. R. Byer, T. C. Hufnagel, and K. A. Dahmen, Phys. Rev. Lett. **112**, 155501 (2014).
[26]G. Tsekenis, J. T. Uhl, N. Goldenfeld, and K. A. Dahmen, Europhys. Lett. **101**, 36003 (2013).
[27]K. A. Dahmen, Y. Ben-Zion, and J. T. Uhl, Nat. Phys. **7**, 554 (2011).
[28]K. Martens, L. Bocquet, and J.-L. Barrat, Soft Matter **8**, 4197 (2012).
[29]O.-A. Adami, Ž. L. Jelić, C. Xue, M. Abdel-Hafiez, B. Hackens, V. V. Moshchalkov, M. V. Milošević, J. Van de Vondel, and A. V. Silhanek, Phys. Rev. B **92**, 134506 (2015).
[30]Z. Zhao, X. Ding, J. Sun, and E. K. H. Salje, J. Phys.: Condens. Matter **26**, 142201 (2014).
[31]E. K. H. Salje, X. Ding, and Z. Zhao, Phys. Rev. B **83**, 104109 (2011).
[32]S. Plimpton, J. Comput. Phys. **117**, 1 (1995).
[33]S. Nosé, J. Chem. Phys. **81**, 511 (1984).
[34]W. G. Hoover, Phys. Rev. A **31**, 1695 (1985).
[35]R. J. Harrison and E. K. H. Salje, Appl. Phys. Lett. **97**, 021907 (2010).